

Electronic Supplementary Information

From cubane-assembled Mn-oxo clusters to monodispersed manganese oxide colloidal nanocrystals

Yan He¹, Yang Liu², Huijuan Zheng¹, Zhen Xiang¹, Zheng Zhou^{1*}, Fengting Geng³, Longlong Geng³, Evgeny V. Dikarev^{4*}, Haixiang Han^{1*}

¹*Interdisciplinary Materials Research Center, School of Materials Science and Engineering, Tongji University, Shanghai 201804, China.*

²*Department of Material Science, Fudan University, Shanghai 200433, China.*

³*Shandong Provincial Key Laboratory of Monocrystalline Silicon Semiconductor Materials and Technology, College of Chemistry and Chemical Engineering, Dezhou University, Dezhou 253023, China.*

⁴*Department of Chemistry, University at Albany, Albany, New York 12222, United States.*

*Author to whom correspondence should be addressed.

E-mail: zhouzheng@tongji.edu.cn, edikarev@albany.edu and
hxhan@tongji.edu.cn

Contents

Experimental section & general procedures	3
Synthetic procedures	5
Crystal growth	6
X-ray crystallographic procedures.....	7
Solid state structures of [Mn₁₈-Ac] and [Mn₁₈-Piv]	9
Magnetic properties.....	19
X-ray photoelectron spectroscopy (XPS).....	20
Synthesis and analysis of Mn ₃ O ₄ hausmannite nanocrystals	22
Theoretical calculations.....	24
References.....	35

Experimental section & general procedures

All manipulations were carried out in a dry, oxygen-free argon atmosphere by employing standard Schlenk and glove box techniques. Manganese(II) perchlorate hexahydrate ($\text{Mn}(\text{ClO}_4)_2 \cdot 6\text{H}_2\text{O}$, 99%), manganese(III) acetate dihydrate ($\text{Mn}(\text{OOCCH}_3)_3 \cdot 2\text{H}_2\text{O}$, 99%), pivalic acid ($\text{C}(\text{CH}_3)_3\text{COOH}$, 99%), triethylamine (Et_3N , 99.9%), pyridine (py, 99.5%), methanol (99.9%), ethanol (99.9%), acetonitrile (99.9%), dichloromethane (99.9%) and hexane (99.9%) were purchased from Adamas and used upon received.

XPS: X-ray photoelectron spectroscopy (XPS) was recorded on Thermo Scientific K-Alpha spectrometer. Samples were grounded into powder and compressed to flakes, which were then attached to sample plate. Then samples were placed in Thermo Scientific $\text{K}\alpha$ XPS instrument sample chamber and vacuumed to 2.0×10^{-7} mBar. The setting parameters of X-ray irradiation were: Al $\text{K}\alpha$ radiation ($h\nu = 1486.6$ eV), 400 μm beam spot, 12 kV working voltage and 6 mA filament current. Survey spectrum was scanned at the energy of 150 eV with 1 eV per step. High-resolution spectra were scanned at the energy of 50 eV with 0.1 eV per step.

XANES: Mn K -edge X-ray absorption near edge spectroscopy (XANES) data were collected using a bench-top easyXAFS300+ instrument (easyXAFS, LLC). Spectra were collected using Si (110) spherically bent crystal analyzer and Ag anode X-ray tube, respectively. Spectra were deadtime corrected and the energy was calibrated using a Mn mesh standard.

Magnetic measurement: Solid-state DC susceptibility of clusters was measured by American Quantum Design PPMS-9-VSM accessories. The magnetic field was set as 0.1 T; the vibrating frequency was 40 Hz, vibration amplitude was 0.5 mm; the resolution was about 3.5×10^{-6} emu; the temperature range was 5–300 K; the maximum magnetic moment was 120 emu. The program was executed and the M-T data were collected in the temperature range of 5–300 K.

Photocatalytic properties: The photocatalytic activities of the synthesized clusters were evaluated by degrading tetracycline (TC) with peroxomonosulfate (PMS) as the oxidant. Typically, the cluster (2 mg) was dispersed into a 20 ppm TC solution (10 mL) and stirred for 10 min in a parallel photochemical reaction device (CEL-LAB200E7, Beijing Zhongguo Jinyuan Science and Technology Co., Ltd.) to reach the adsorption-desorption equilibrium. Then PMS (2 mg) was added and irradiated with a visible light from a 30 W LED lamp ($400 \text{ nm} < \lambda < 760 \text{ nm}$) to initiate the photocatalytic degradation reaction. During the reaction progress, 1 mL of the solution was taken and centrifuged at regular intervals, and the concentration of the supernatant was analyzed by UV-visible spectrophotometer. The degradation efficiency of the synthesized catalyst was determined through A_t/A_0 , and the photocatalytic rate constant was calculated using the equation:

$$\ln\left(\frac{A_t}{A_0}\right) = -kt$$

where A_0 and A_t represent the absorbance of TC solution at time 0 and t, respectively.

TEM: Transmission electron microscope (TEM) images were collected on a JEOL JEM-2010 at an accelerating voltage of 200 kV. TEM grids were prepared by dropping a dilute nanocrystal dispersion in CH_2Cl_2 onto a carbon-coated copper TEM grid and allowing the sample to dry under air.

X-ray powder diffraction: X-ray powder diffraction data were collected on a Bruker D2 Advance diffractometer (Cu $\text{K}\alpha$ focusing Goebel Mirror, LynxEye one-dimensional detector,

step of 0.01° , 2θ , $20\text{ }^\circ\text{C}$). The examined crystalline samples were ground, spread on the frosted sample stage and placed into the dome-shaped airtight zero-background holders. Le Bail fit for the powder diffraction patterns has been performed using TOPAS, version 7.13 software package (Bruker AXS, 2006).

Synthetic procedures

Mn₁₈O₁₀(OOCMe)₁₂(OMe)₁₄(py)₂ ([Mn₁₈-Ac])

Mn(OAc)₃·2H₂O (54 mg, 0.2 mmol) was loaded into a 50 mL tube-like Schlenk flask followed by the addition of 5 mL MeCN, 0.5 mL pyridine and 0.2 mL Et₃N. The solution was heated at 60 °C and stirred for 4 h. After the solution cooled down to room temperature, 5 mL MeOH was added, and the resultant dark solution was further stirred for 2 h at room temperature. The solvent was then evaporated off, and the brownish residue was washed with Et₂O for several times. The final residue was obtained after being vacuum dried for several hours to yield a pure, fine brownish powder. The yield is *ca.* 42 %.

Mn₁₈O₁₄(OOCCMe₃)₈(OMe)₁₄(MeOH)₅(py) ([Mn₁₈-Piv])

Mn(ClO₄)₂·6H₂O (108 mg, 0.3 mmol) and C(CH₃)₃COOH (30.6 mg, 0.3 mmol) were loaded into a 50 mL tube-like Schlenk flask, which was followed by the addition of 5 mL MeOH to dissolve all reagents. After that, 0.5 mL pyridine and 0.2 mL Et₃N were added resulting in an orange solution. After stirring in the open air for 1 h, the color of the solution slowly turned from orange to dark brown. The brown solution was then evaporated under vacuum at room temperature to leave a brownish residue. The residue was then washed with hexanes for several times and vacuum-dried for several hours to yield a pure, dry brownish final product. The yield is *ca.* 66 %.

1-Mn₃O₄ nanocrystals

50 mg of [Mn₁₈-Ac] powder was dispersed in 10 mL oleylamine and 2 mL water was added to the suspension. The mixture was slowly heated to 220 °C, and kept at this temperature for 9 hours, and then cooled down to room temperature. After staying undisturbed at room temperature for 10 min, brown precipitate and light-colored supernatant were yielded. The mixture was centrifuged, and the supernatant was discarded. The solid residue was washed with hexanes for several times. The yield is *ca.* 34 %.

2-Mn₃O₄ nanocrystals

50 mg of [Mn₁₈-Piv] powder was dispersed in 10 mL oleylamine and 2 mL water was added to the suspension. The mixture was slowly heated to 220 °C, and kept at this temperature for 9 hours and then cooled down to room temperature. After staying undisturbed at room temperature for 10 min, brown precipitate and light-colored supernatant were yielded. The mixture was centrifuged, and the supernatant was discarded. The solid residue was washed with hexanes for several times. The yield is *ca.* 38 %.

Crystal growth

Brown plate-like crystals of **[Mn₁₈-Ac]** and brown block crystals of **[Mn₁₈-Piv]** suitable for X-ray single crystal structural measurements were obtained through a low-temperature crystallization process. The saturated solutions of **[Mn₁₈-Ac]** in MeOH/MeCN (v:v = 1:1) and **[Mn₁₈-Piv]** in MeOH were sealed in glass vials and stored in a 5 °C fridge for one or two weeks to promote crystal growth.

Table S1. Single crystal growth conditions.

Compound	[Mn₁₈-Ac]	[Mn₁₈-Piv]
Shape	Plate	Block
Color	Brown	Brown
Method	Low temp solution crystallization	Low temp solution crystallization
Time	2 weeks	1 week
Temperature	5 °C	5 °C

X-ray crystallographic procedures

Data collection of **[Mn₁₈-Ac]** was performed on a Bruker D8 VENTURE X-ray diffractometer with PHOTON 100 CMOS detector equipped with a Cu-target. The Incoatec microfocus source μ S X-ray tube ($\lambda = 1.5406 \text{ \AA}$) at $T = 160 \text{ K}$. Data collection of **[Mn₁₈-Piv]** was performed on a Rigaku XtaLAB-Synergy-R X-ray diffractometer with PHOTON 100 CMOS detector equipped with a Mo-target. The Incoatec microfocus source μ S X-ray tube ($\lambda = 0.71073 \text{ \AA}$) at $T = 150 \text{ K}$. Data reduction and integration were performed with the Bruker software package SAINT (version 8.38A).¹ Data were corrected for absorption effects using the empirical methods as implemented in SADABS (version 2016/2).² The structure was solved by SHELXT³ and refined by full-matrix least-squares procedures using the Bruker SHELXTL (version 2018/3) software package through the OLEX2 graphical interface.⁴ All non-hydrogen atoms were refined anisotropically. The H-atoms were included at calculated positions and refined as riders, with $U_{\text{iso}}(\text{H}) = 1.2 U_{\text{eq}}(\text{C})$. The anisotropic displacement parameters in the direction of the bonds were restrained to be equal with a standard uncertainty of 0.004 \AA^2 . They were also restrained to have the same U_{ij} components, with a standard uncertainty of 0.01 \AA^2 . Further crystal and data collection details are listed in Table S2.

Table S2. Crystal data and structure refinement parameters for **[Mn₁₈-Ac]** and **[Mn₁₈-Piv]**.

Compound	[Mn₁₈-Ac]	[Mn₁₈-Piv]
CCDC	2325204	2325203
Formula weight	2450.12	2727.72
Temperature (K)	160	150
Wavelength (Å)	1.54178	0.71073
Crystal system	Triclinic	Monoclinic
Space group	<i>P</i> 1̄	<i>P</i> 2 ₁ /c
<i>a</i> (Å)	10.4312(5)	16.7116(5)
<i>b</i> (Å)	13.1605(6)	31.6354(5)
<i>c</i> (Å)	16.2948(8)	23.4460(5)
α (°)	106.181(3)	90
β (°)	99.194(4)	110.465(3)
γ (°)	90.133(4)	90
<i>V</i> (Å ³)	2118.14(18)	11613.1(5)
<i>Z</i>	1	4
ρ_{calcd} (g·cm ⁻³)	1.971	1.707
μ (mm ⁻¹)	21.854	1.958
<i>F</i> (000)	1260	6136
θ range for data collection (°)	2.864–72.628	1.963–30.820
Reflections collected	32244	153634
Independent reflections	8321 ($R_{\text{int}} = 0.1055$)	30057 ($R_{\text{int}} = 0.1450$)
Transmission factors (min/max)	0.779/0.828	0.798/0.891
Data/restraints/params.	8321/396/518	30057/781/1411
<i>R</i> 1, ^a <i>wR</i> 2 ^b (<i>I</i> > 2σ(<i>I</i>))	0.0707/0.1820	0.0958/0.2399
<i>R</i> 1, ^a <i>wR</i> 2 ^b (all data)	0.1306/0.2192	0.1447/0.2714
Quality-of-fit ^c	0.928	1.028
Largest diff. peak and hole (e·Å ⁻³)	1.397 and -1.464	1.915 and -1.432

^a $R_1 = \sum ||F_o| - |F_c|| / \sum |F_o|$. ^b $wR2 = [\sum [w(F_o^2 - F_c^2)^2] / \sum [w(F_o^2)^2]]$.^cQuality-of-fit = $[\sum [w(F_o^2 - F_c^2)^2] / (N_{\text{obs}} - N_{\text{params}})]^{1/2}$, based on all data.

Solid state structures of $[\text{Mn}_{18}\text{-Ac}]$ and $[\text{Mn}_{18}\text{-Piv}]$

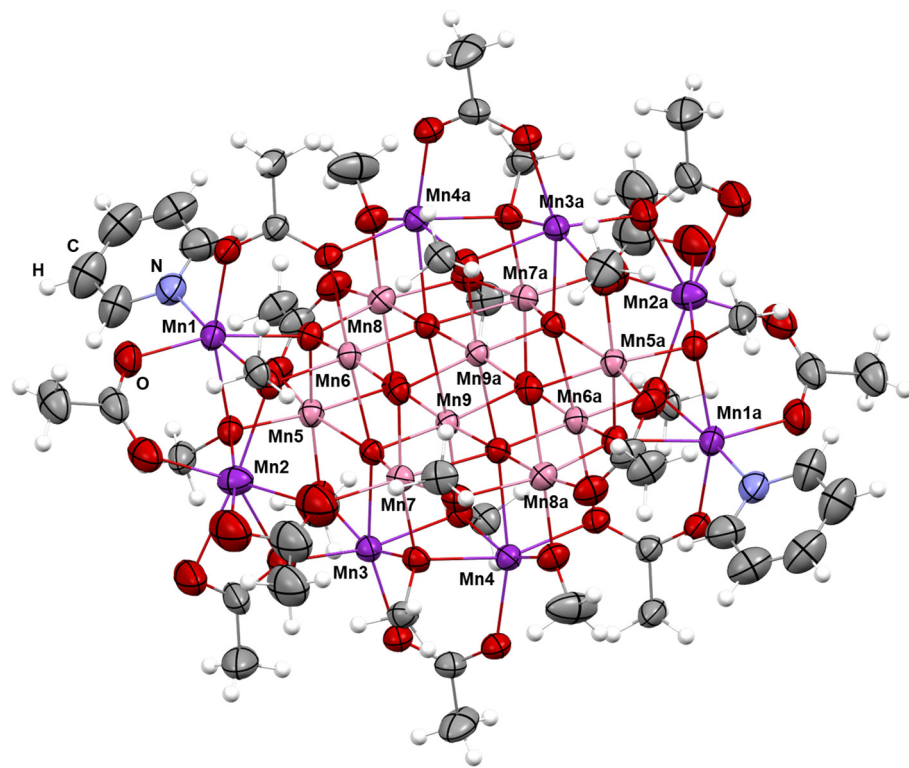


Figure S1. Solid state structure of $[\text{Mn}_{18}\text{-Ac}]$ drawn with thermal ellipsoids at the 40% probability level. Hydrogen atoms are represented by spheres of arbitrary radius. Only metal cations are labeled. Mn^{II}, purple; Mn^{III}, pink; O, red; N, blue; C, grey; H, white.

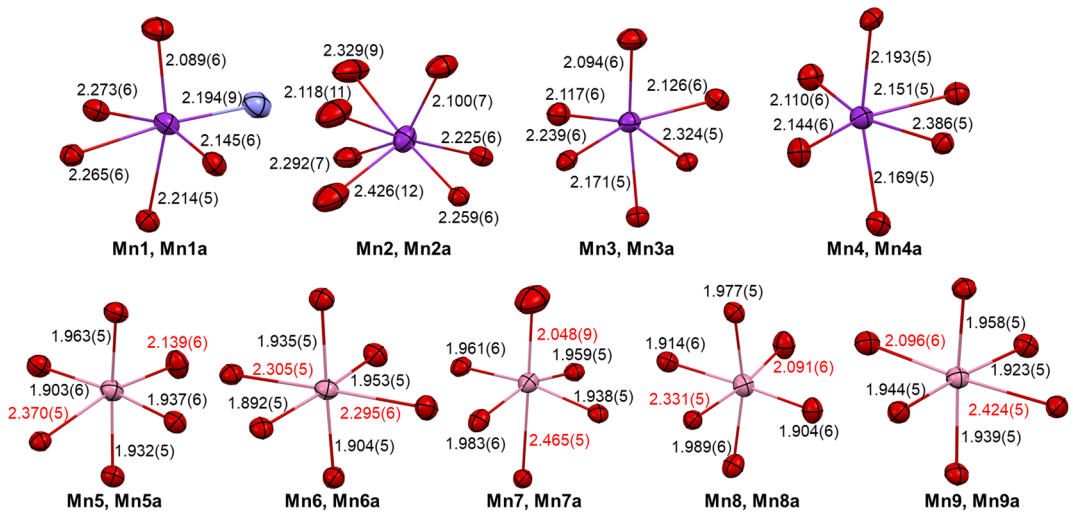


Figure S2. Bond lengths (Å) for the Mn ions with nonmetal atoms in structure **[Mn₁₈-Ac]**. Red labels represent the Jahn-Teller distorted Mn–O bonds.

Table S3. Average bond lengths (Å), oxidation states and JT distortion of all the Mn atoms in the structure of [Mn₁₈-Ac].

Mn atoms	Avg. Mn–O length	Oxidation states of Mn	Jahn-Teller effect
Mn1, Mn1a	2.197	+2	\
Mn2, Mn2a	2.250	+2	\
Mn3, Mn3a	2.179	+2	\
Mn4, Mn4a	2.192	+2	\
Mn5, Mn5a	2.041	+3	Elongated
Mn6, Mn6a	2.034	+3	Elongated
Mn7, Mn7a	2.047	+3	Elongated
Mn8, Mn8a	2.047	+3	Elongated
Mn9, Mn9a	2.059	+3	Elongated

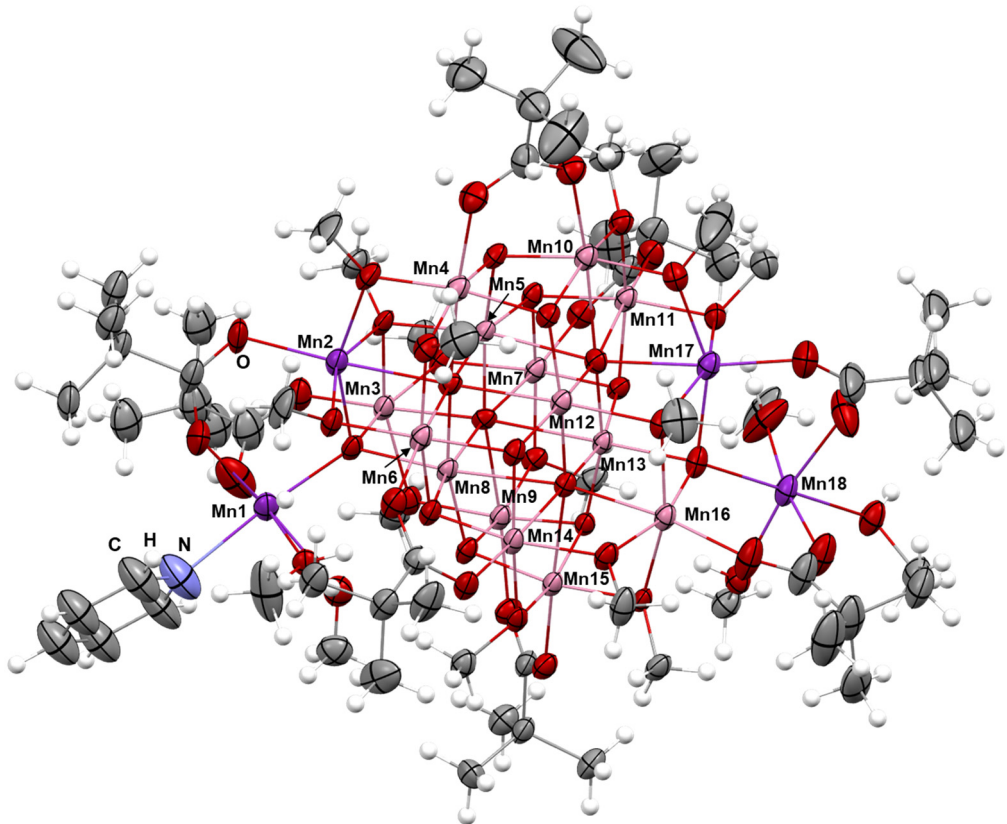


Figure S3. Solid state structure of **[Mn₁₈-Piv]** drawn with thermal ellipsoids at the 40% probability level. Hydrogen atoms are represented by spheres of arbitrary radius. Only metal cations are labeled. Mn^{II}, purple; Mn^{III}, pink; O, red; N, blue; C, grey; H, white.

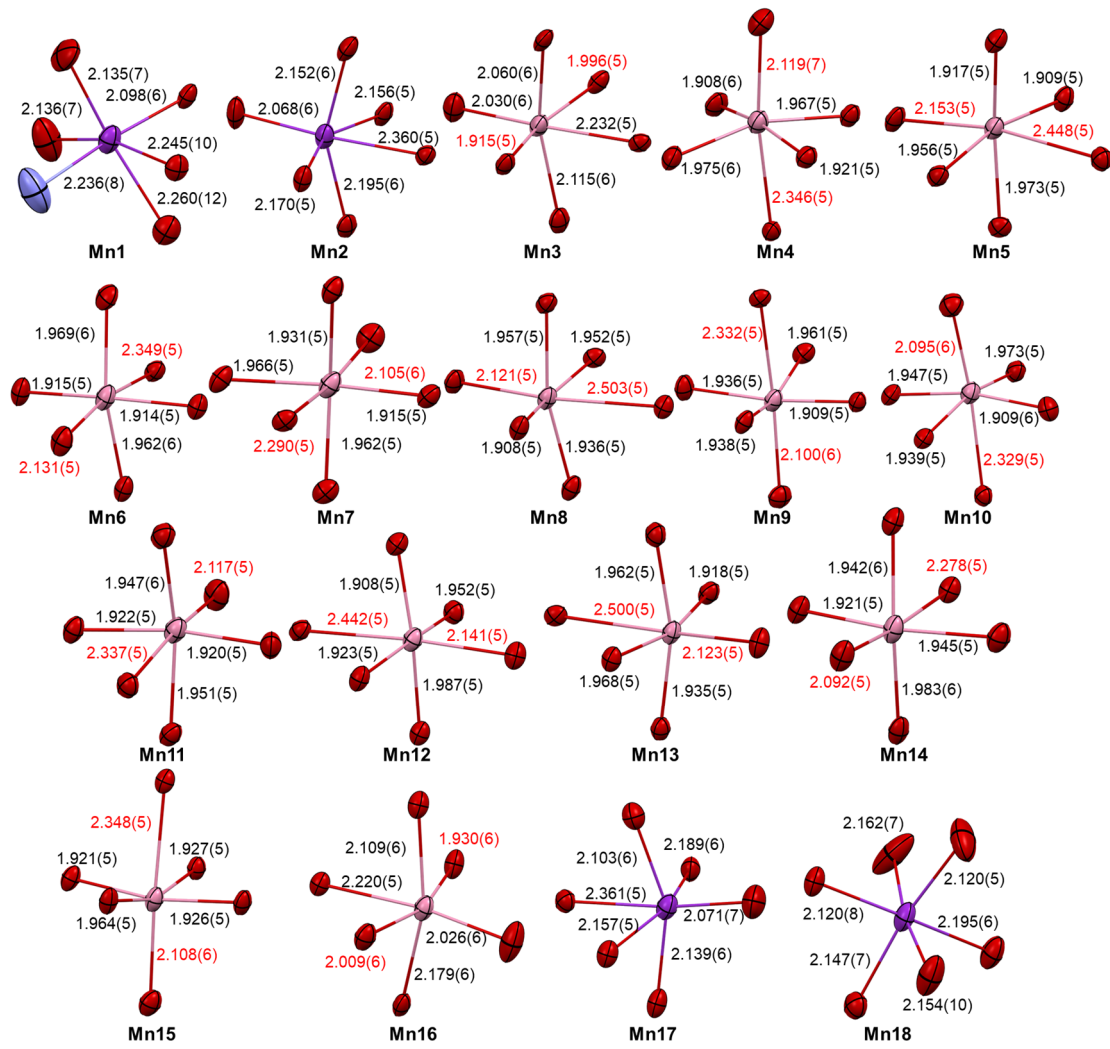


Figure S4. Bond lengths (Å) for the Mn ions with nonmetal atoms in structure of **[Mn₁₈-Piv]**. Red labels represent the Jahn-Teller distorted Mn–O bonds.

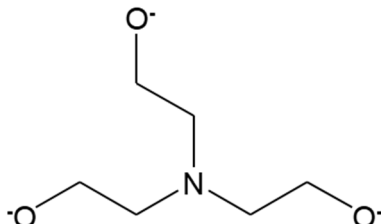
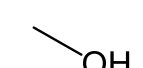
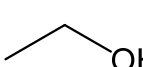
Table S4. Average bond lengths (Å), oxidation states and JT distortion for the Mn atoms in the structure of [Mn₁₈-Piv].

Mn atoms	Avg. Mn–O length	Oxidation states of Mn	Jahn-Teller effect
Mn1	2.174	+2	\
Mn2	2.183	+2	\
Mn3	2.058	+3	Compressed
Mn4	2.038	+3	Elongated
Mn5	2.060	+3	Elongated
Mn6	2.037	+3	Elongated
Mn7	2.027	+3	Elongated
Mn8	2.065	+3	Elongated
Mn9	2.027	+3	Elongated
Mn10	2.031	+3	Elongated
Mn11	2.032	+3	Elongated
Mn12	2.060	+3	Elongated
Mn13	2.068	+3	Elongated
Mn14	2.026	+3	Elongated
Mn15	2.032	+3	Elongated
Mn16	2.079	+3	Compressed
Mn17	2.169	+2	\
Mn18	2.149	+2	\

Table S5. Different types of ligands utilized in the reported Mn-oxo clusters.

Type	Schematic structure	Ligand
Diketonates		thd ⁵
		dbm ⁵⁻⁷
Carboxylates		OOCMe ⁸⁻¹²
		OOCEt ¹³
		OOC <i>t</i> Bu ¹⁴⁻¹⁶
		OOCCH ₂ <i>t</i> Bu ^{17, 18}
		OOC <i>t</i> Pe ¹⁹

		dma ²⁰
		ndc ²¹
		OOCPh ^{7, 12, 21}
Alkoxides		OMe ^{5, 6, 9, 11, 15, 22}
		OEt (deprotonated) ^{5, 10}
		hmp ^{23, 24}
		pdm ^{8, 23}
		dpkd ¹⁶

		tea ^{25, 26}
		py ²⁷
Neutral molecules		MeOH ^{5, 11, 28}
		EtOH ^{5, 10}
		H ₂ O ^{9, 11, 15, 17, 18}

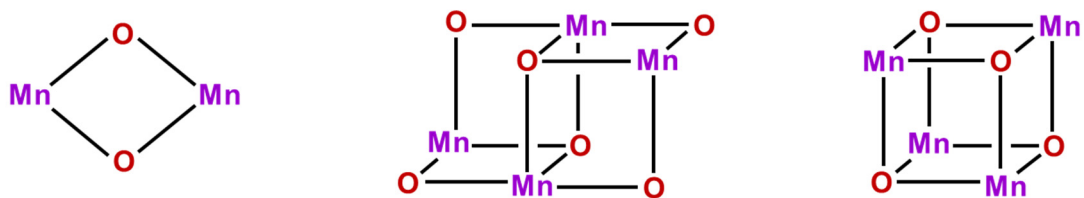


Figure S5. Schematic representations of the $[\text{Mn}_2\text{O}_2]$ (left), $[\text{Mn}_4\text{O}_6]$ (middle) and $[\text{Mn}_4\text{O}_4]$ (right) units that have been found both in Mn-oxo clusters and manganese oxide bulk materials.

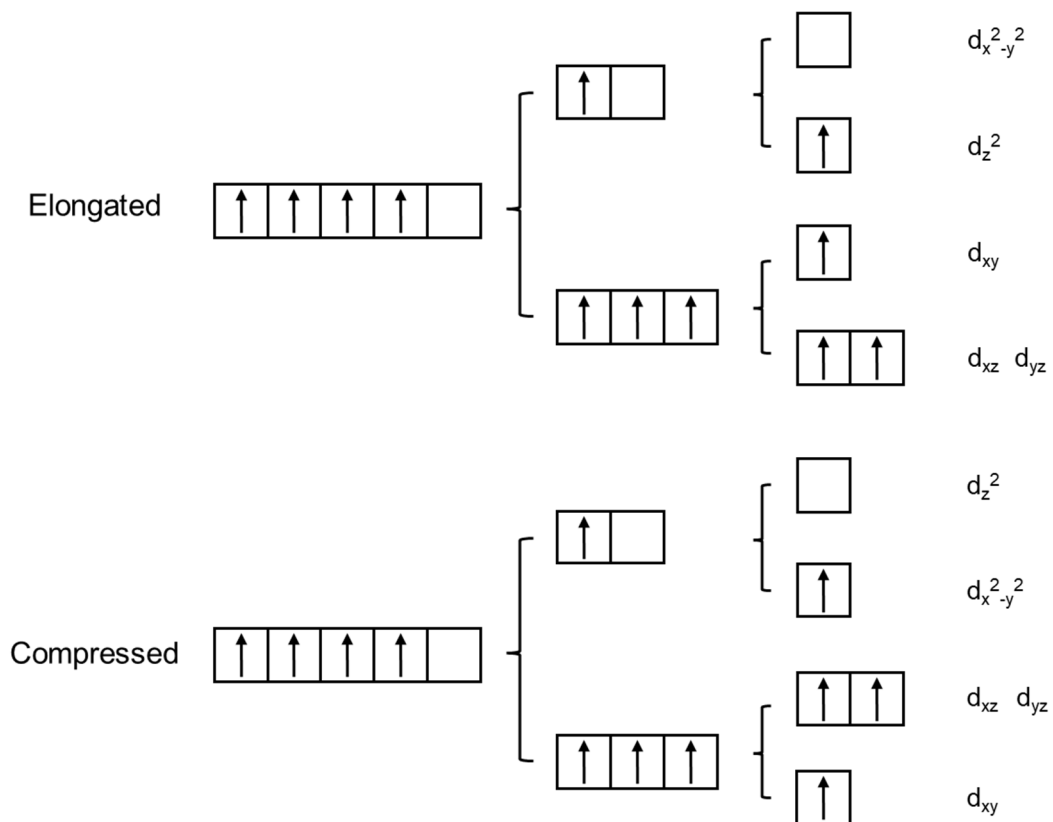


Figure S6. Electronic configurations of Mn^{III} $3d$ orbitals in elongated (top) and compressed (bottom) Jahn-Tell manifestations.

Magnetic properties

The magnetic properties of clusters **[Mn₁₈-Ac]** and **[Mn₁₈-Piv]** were studied in a temperature range of 5–300 K at $H = 0.1$ T using direct-current (DC) magnet susceptibility measurements in the solid state. At room temperature, the $\chi_M T$ values of **[Mn₁₈-Ac]** and **[Mn₁₈-Piv]** are 39.05 and 116.46 cm³·K·mol⁻¹, respectively, and the large difference reflects different ratios of Mn^{II} to Mn^{III} ions in two structures. Upon cooling, the $\chi_M T$ values remain constant up to around 40 K, followed by a sharp decrease to reach the final values of 19.54 and 33.38 cm³·K·mol⁻¹ at 5 K, respectively, where $S = 12/2$ and $16/2$ can be calculated for **[Mn₁₈-Ac]** and **[Mn₁₈-Piv]**. The increase of $\chi_M T$ values around 40 K is attributed to the higher ferromagnetic interactions between Mn ions in both clusters. To be specific, the $\chi_M T$ value is 74.04 cm³·K·mol⁻¹ for **[Mn₁₈-Ac]** (at 32 K), in contrast, it reaches a value of 186.52 cm³·K·mol⁻¹ at 46 K. The observed higher $\chi_M T$ values for **[Mn₁₈-Piv]** reflects its higher Mn spins in the structure, which is consistent with the crystallographic and DFT calculations results.

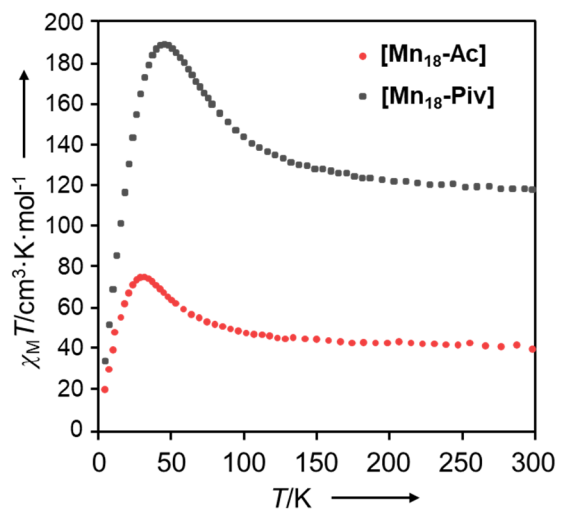


Figure S7. Temperature dependence of the $\chi_M T$ product for **[Mn₁₈-Ac]** and **[Mn₁₈-Piv]** at 0.1 T (χ_M , the DC magnetic susceptibility, defined as M/H per mole of complex).

X-ray photoelectron spectroscopy (XPS)

XPS is a sensitive surface technology that has been widely utilized to determine the binding energy for the elements of interest. Based on the characteristic binding energies of the inner shell electrons, the absolute (typically, extremely difficult) and variation of the oxidation states for metals can be determined. Unfortunately, the Mn $2p_{3/2}$ and Mn $2p_{1/2}$ peaks for Mn^{II} and Mn^{III} cannot be clearly distinguished as they both appear at 641.4 eV and 653.2 eV, respectively.²⁹ But the observation of shake-up peak at 647 eV is indicative of the presence of Mn^{II}, since that signal is absent in Mn^{III} species. In the Mn 2p spectra of **[Mn₁₈-Ac]** and **[Mn₁₈-Piv]** (ESI, Figure S8a), their Mn $2p_{3/2}$ and Mn $2p_{1/2}$ peaks appear at almost identical positions with the splitting energies being all close to 11.8 eV. In addition, shake-up peaks can be observed in the spectra of **[Mn₁₈-Ac]** and **[Mn₁₈-Piv]**. However, the intensities of the shake-up peaks are quite low and there is no significant difference between them. It should be noted here that taking the overall peak profile into account, a single-phase simulation for **[Mn₁₈-Ac]** and **[Mn₁₈-Piv]** single-phase fitting (ESI, Figure S9a, S9b) seems to be less reasonable than introducing the two-phase fitting (ESI, Figure S8b, S8c), which corresponds to the Mn^{II} and Mn^{III} in their structures. In addition, another XPS signature that can be used to discern Mn^{II} and Mn^{III} may be their respective Mn 3s orbitals, where the splitting energy for Mn^{II} (5.9 eV) is usually smaller than that for Mn^{III} (5.5 eV).²⁹ The high-resolution Mn 3s spectra of **[Mn₁₈-Ac]** and **[Mn₁₈-Piv]** (ESI, Figure S9c), however, show close and indiscernible splitting energies, which cannot be reliably applied to distinguish Mn^{II} and Mn^{III}.³⁰

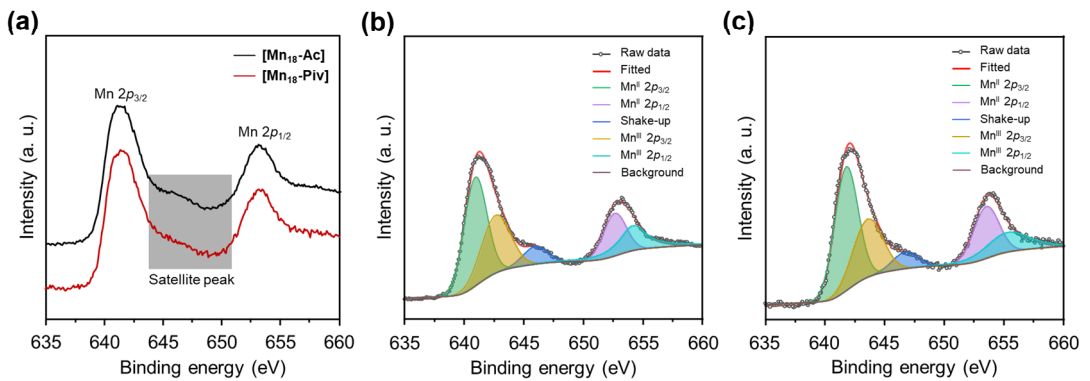


Figure S8. High-resolution XPS spectra for Mn $2p$ orbitals of $[\text{Mn}_{18}\text{-Ac}]$ and $[\text{Mn}_{18}\text{-Piv}]$ (a). The Mn^{II} + Mn^{III} double-phase simulation of high-resolution XPS spectra for Mn $2p$ orbitals for $[\text{Mn}_{18}\text{-Ac}]$ (b) and $[\text{Mn}_{18}\text{-Piv}]$ (c).

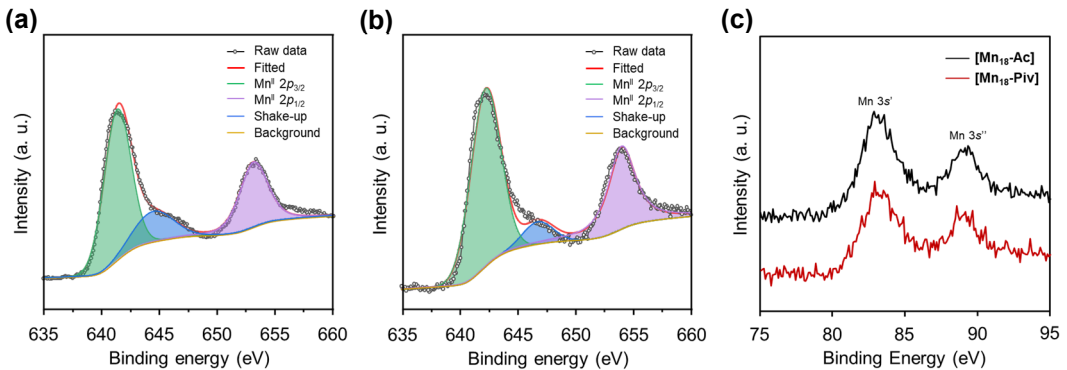


Figure S9. Mn^{II} single-phase simulation of high-resolution XPS spectrum for Mn $2p$ orbitals in $[\text{Mn}_{18}\text{-Ac}]$ (a) and $[\text{Mn}_{18}\text{-Piv}]$ (b). High-resolution XPS spectrum for Mn $3s$ orbitals in $[\text{Mn}_{18}\text{-Ac}]$ and $[\text{Mn}_{18}\text{-Piv}]$ (c).

Synthesis and analysis of Mn_3O_4 hausmannite nanocrystals

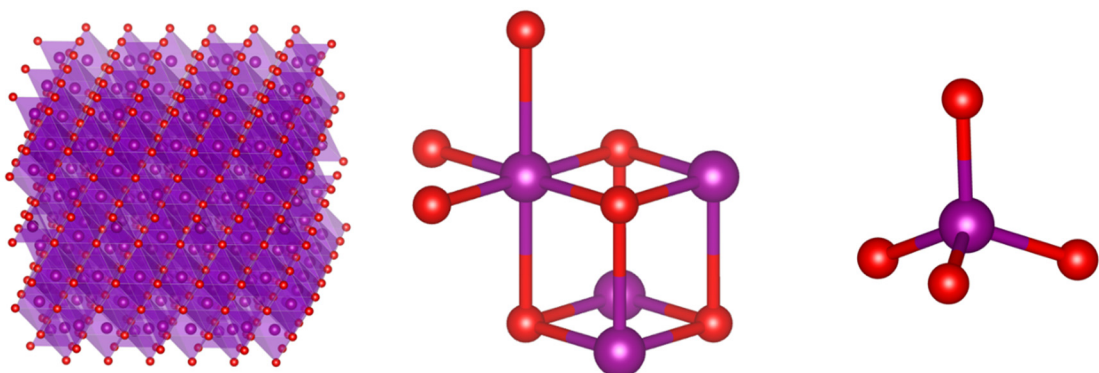


Figure S10. Crystal structure of Mn_3O_4 hausmannite (left) with the $[\text{Mn}_4\text{O}_4]$ cubic (center) and $[\text{MnO}_4]$ tetrahedron (right) constituent units.

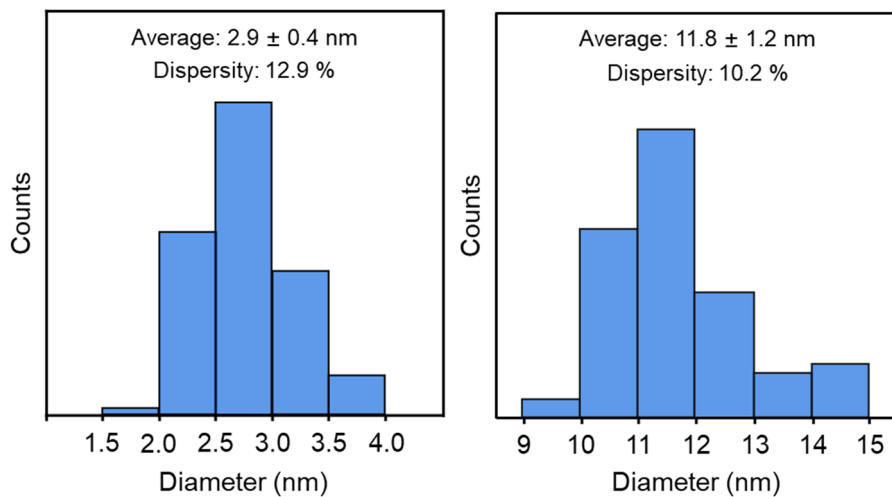


Figure S11. Histograms of the statistical size distribution of Mn_3O_4 nanocrystals obtained from $[\text{Mn}_{18}\text{-Ac}]$ (left) and $[\text{Mn}_{18}\text{-Piv}]$ (right) precursors.

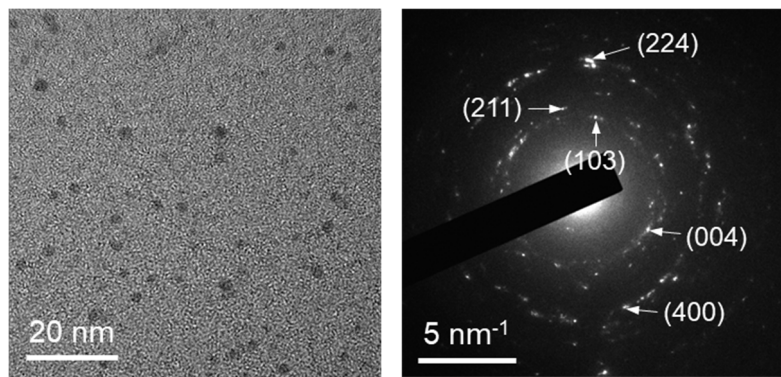


Figure S12. TEM micrographs of the **1-Mn₃O₄** nanocrystals obtained from **[Mn₁₈-Ac]** (left) precursor and the corresponding ring electron diffraction pattern (right).

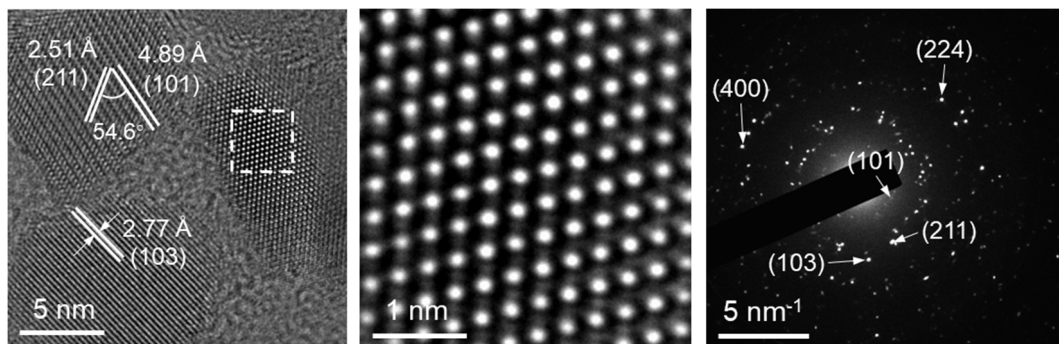


Figure S13. TEM micrographs of the **2-Mn₃O₄** nanocrystals obtained from **[Mn₁₈-Piv]** (left and middle) precursor and the corresponding ring electron diffraction pattern (right). The middle figure is the micrograph of the selected area inside the dashed box in the left micrograph. Figure 7f in manuscript is the fast Fourier transform (FFT) pattern of the middle figure.

Theoretical calculations

All calculations were performed with ORCA 5.1.0.³¹ The geometry optimization of all structures were performed using PBE hybrid functional³² under def2-SVP level,³³ and the energy was calculated using the same method under def2-TZVP level.³³ For Mn₁₈ clusters, the geometries were extracted from crystal structures and the spin numbers were calculated from the SQUID experiments, that are S = 12/2 for [Mn₁₈-Ac] and S = 16/2 for [Mn₁₈-Piv]. The MO diagrams were generated by GaussView 6.0. The PDOS plot was generated by Multiwfn 3.8.³⁴ The oxidation states of Mn ions in [Mn₁₈-Ac] and [Mn₁₈-Piv] were calculated in Multiwfn using localized orbital bonding analysis method.³⁵

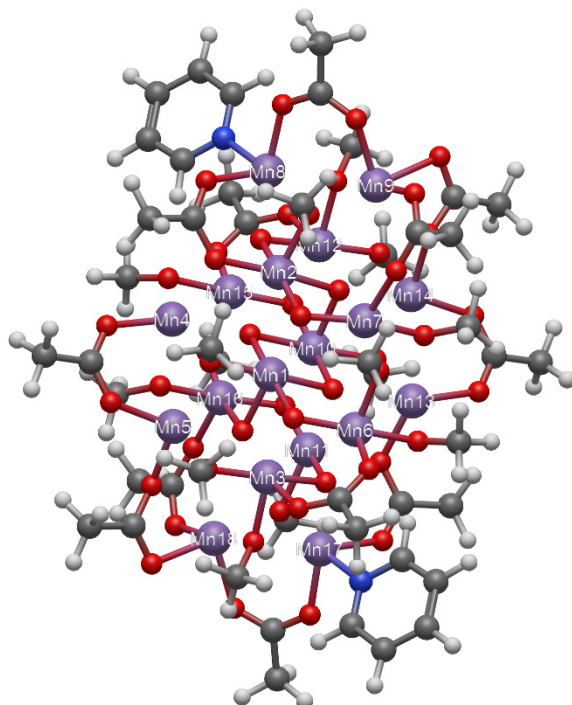


Table S6. Oxidation state calculations of Mn atoms in [Mn₁₈-Ac] along with a labeling scheme.

Atomic No.	Oxidation state	Atomic No.	Oxidation state
1	+3	10	+3
2	+3	11	+3
3	+3	12	+3
4	+2	13	+2
5	+2	14	+2
6	+3	15	+3
7	+3	16	+3
8	+2	17	+2
9	+2	18	+2

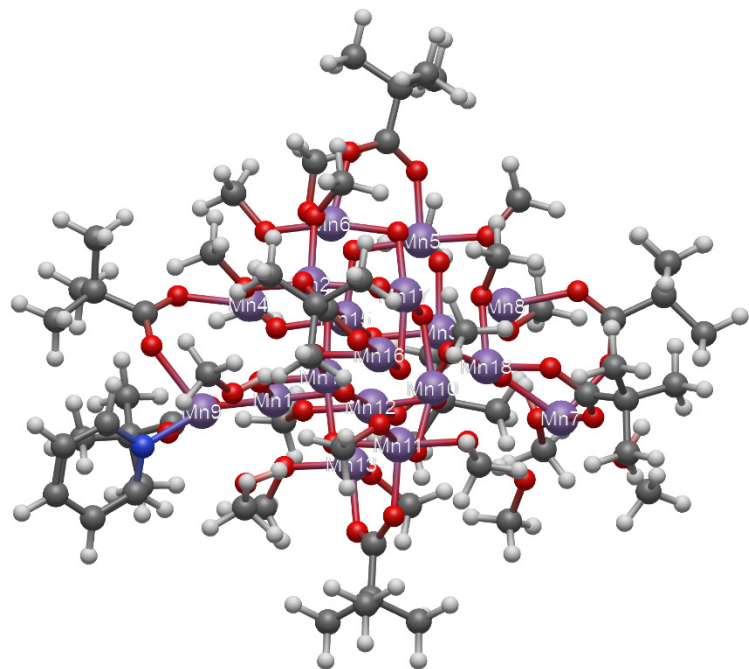


Table S7. Oxidation state calculations of Mn atoms in **[Mn₁₈-Piv]** along with a labeling scheme.

Atomic No.	Oxidation state	Atomic No.	Oxidation state
1	+3	10	+3
2	+3	11	+3
3	+3	12	+3
4	+2	13	+3
5	+3	14	+3
6	+3	15	+3
7	+2	16	+3
8	+2	17	+3
9	+2	18	+3

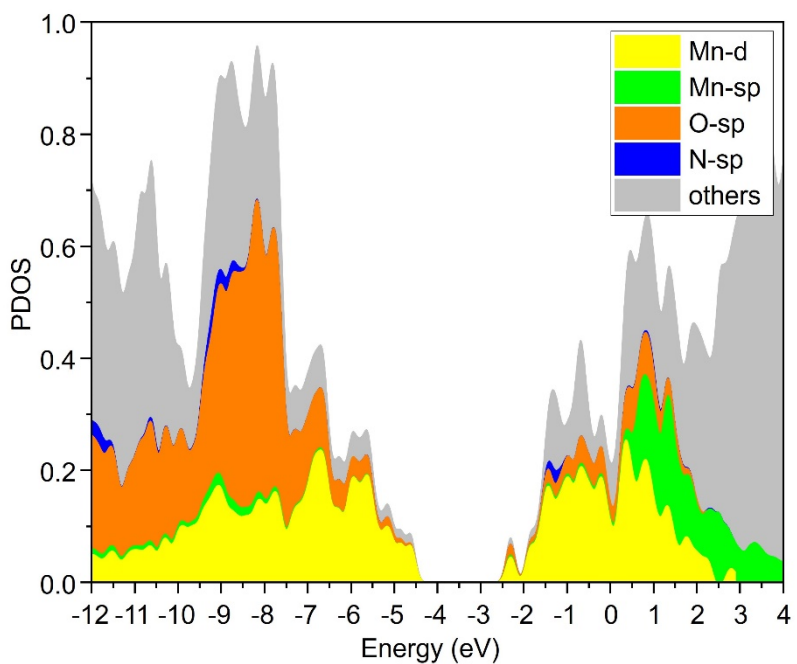


Figure S14. Partial density of states (PDOS) of alpha orbitals in $[\text{Mn}_{18}\text{-Ac}]$.

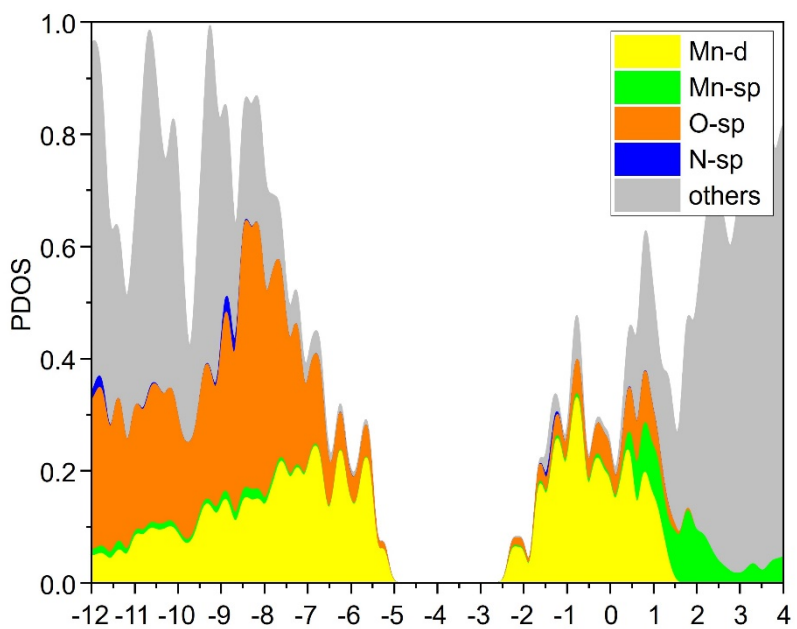


Figure S15. Partial density of states (PDOS) of alpha orbitals in $[\text{Mn}_{18}\text{-Piv}]$.

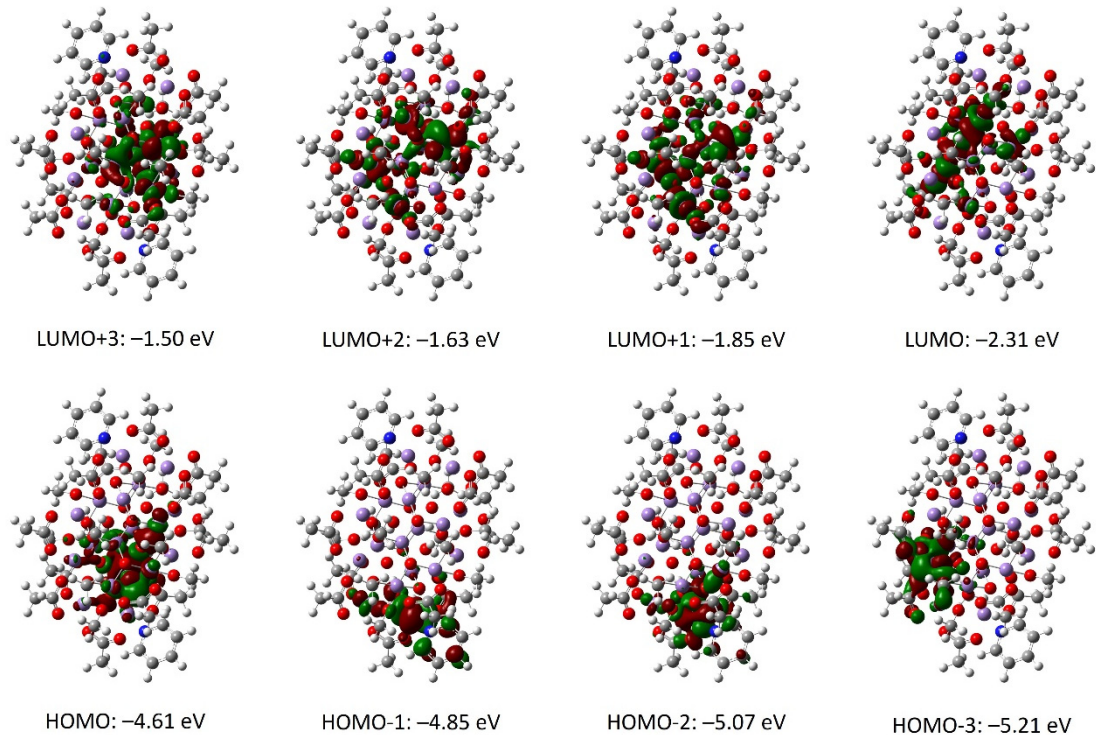


Figure S16. Selected active molecular orbitals in **[Mn₁₈-Ac]**.

Table S8. Orbital composition analysis by Hirschfeld method in **[Mn₁₈-Ac]**.

MO	Orbital No.	Contributions from Mn atoms
LUMO+3	622a	Mn7: 39.0%, Mn16: 18.9%, Mn2: 7.0%, Mn3: 6.2%
LUMO+2	621a	Mn16: 24.6%, Mn7: 20.7%, Mn3: 16.2%, Mn1: 4.2%
LUMO+1	620a	Mn16: 42.7%, Mn2: 22.7%
LUMO	619a	Mn11: 51.7%
HOMO	618a	Mn17: 74.6%
HOMO-1	617a	Mn17: 75.6%
HOMO-2	616a	Mn5: 73.8%
HOMO-3	615a	Mn5: 72.5, Mn1: 4.4%

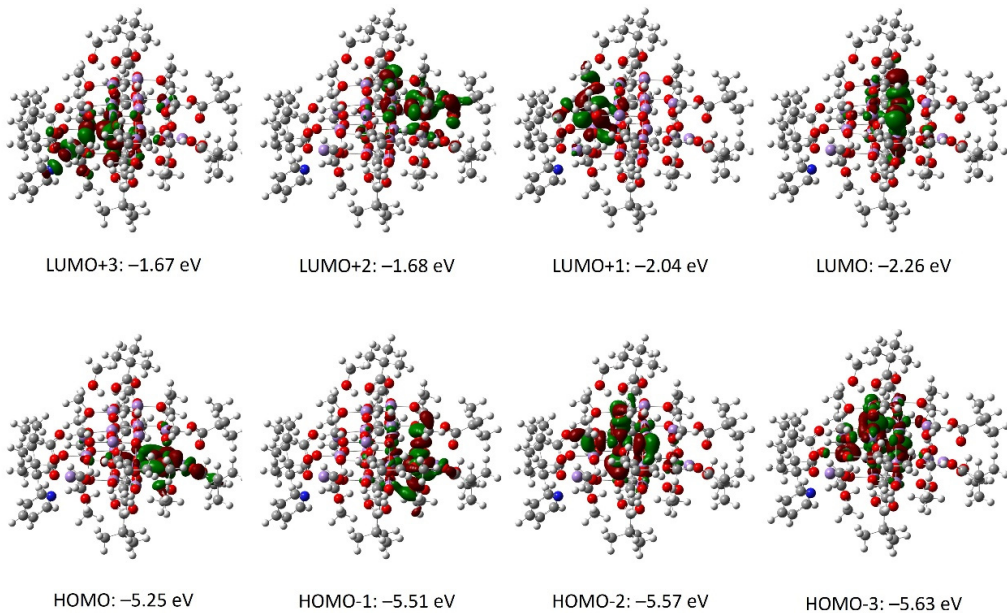


Figure S17. Selected active molecular orbitals in **[Mn₁₈-Piv]**.

Table S9. Orbital composition analysis by Hirschfeld method in **[Mn₁₈-Piv]**.

MO	Orbital No.	Contributions from Mn atoms
LUMO+3	707a	Mn2: 36.5%, Mn17: 17.8, Mn6: 4.0%
LUMO+2	706a	Mn17: 29.1%, Mn18: 18.3%, Mn11: 15.3%
LUMO+1	705a	Mn18: 45.3%, Mn17: 18.7%, Mn11: 4.0%
LUMO	704a	Mn18: 62.2%
HOMO	703a	Mn5: 70.7%
HOMO-1	702a	Mn3: 58.0%, Mn10: 10.0%
HOMO-2	701a	Mn8: 42.1%, Mn15: 15.6, Mn3: 5.1%
HOMO-3	700a	Mn15: 29.3%, Mn4: 28.3%

Table S10. Cartesian coordinates of [Mn₁₈-Ac].

Total energy: -26315.135597754812 Hartree.

Atom	X	Y	Z	Atom	X	Y	Z
Mn	2.761811	4.808272	6.918577	Mn	5.021584	3.900124	8.490542
Mn	2.516990	4.789515	9.837530	Mn	5.329091	3.866519	5.610857
Mn	3.018228	4.703553	3.997005	Mn	4.802144	3.941826	11.442888
Mn	2.681367	7.681251	8.366898	Mn	5.075080	1.031157	7.098729
Mn	2.894648	7.428265	5.300516	Mn	4.886440	1.280410	10.144846
Mn	2.831889	2.331722	5.450997	Mn	4.991671	6.352039	10.002030
Mn	2.377905	2.274589	8.492967	Mn	5.317424	6.411500	7.000141
Mn	2.359597	5.300748	12.736669	Mn	5.486800	3.323060	2.769905
Mn	1.994476	2.217029	12.348577	Mn	5.855872	6.339201	3.055324
O	1.714934	4.005724	8.321966	O	6.091652	4.683277	7.106243
O	2.002093	4.013009	5.419859	O	5.799654	4.653131	9.989505
O	4.180576	3.187048	4.302220	O	3.673109	5.476337	11.152591
O	4.032470	5.598955	5.646345	O	3.683436	3.187363	9.772818
O	1.749110	6.430265	6.858071	O	5.987267	2.228739	8.563077
O	1.483473	6.491757	9.787499	O	6.312863	1.907690	5.671958
O	3.887448	5.589412	8.425402	O	3.937508	3.168697	6.955585
O	3.569010	0.701823	8.536222	O	4.230531	8.015474	6.905934
O	1.422178	3.965333	11.207514	O	6.449797	4.615121	4.132440
O	4.310760	5.077549	2.504943	O	3.566249	3.481345	12.923226
O	1.600176	1.693160	6.789277	O	6.192651	6.976078	8.622211
O	2.034632	6.309791	3.815408	O	5.796945	2.342504	11.607782
O	1.652871	9.380146	7.749980	O	6.071863	-0.701334	7.790966
O	3.823722	0.671438	5.516529	O	3.986671	7.996659	9.985010
O	1.702680	9.110070	5.528523	O	6.073405	-0.392264	10.005529
O	1.187298	6.879988	11.970804	O	6.581483	1.705477	3.467458
O	1.897475	3.673257	2.758709	O	5.944485	4.985730	12.657999
O	1.746688	1.767646	3.944989	O	6.101139	6.905766	11.503371
O	4.304389	8.045578	4.003934	O	3.441331	0.773293	11.467042
O	1.152590	4.912868	14.296324	O	6.741138	3.583756	1.246545
O	0.684606	2.783026	13.817870	O	7.182818	5.756917	1.478244
O	0.878562	1.357292	9.509146	O	6.762589	7.204110	5.976250
N	3.289072	6.694764	13.933510	N	4.554753	2.018537	1.584773
C	0.974622	7.142169	10.785289	C	6.702223	1.272090	4.619401
C	1.506837	2.489918	2.939957	C	6.344340	6.165283	12.496722
C	1.352474	9.717824	6.564958	C	6.402209	-1.018002	8.965476
C	0.020425	4.040426	11.013120	C	7.847577	4.552793	4.360726
H	-0.362614	5.049306	11.232782	H	8.197782	3.508957	4.343615
H	-0.473941	3.331899	11.693370	H	8.374348	5.114343	3.574947
H	-0.228935	3.776265	9.974178	H	8.081467	4.995723	5.341618
C	2.972103	-0.576184	8.656268	C	4.844253	9.280334	6.799019
H	2.038752	-0.609742	8.076483	H	5.770219	9.302682	7.392641
H	2.744906	-0.782399	9.712690	H	5.082602	9.492228	5.745652
H	3.665627	-1.340318	8.273701	H	4.159684	10.057796	7.175480
C	0.347133	6.304160	6.791754	C	7.396496	2.330593	8.586288
H	0.073473	5.529926	6.059482	H	7.696137	3.145674	9.260504
H	-0.095932	7.263358	6.477690	H	7.827730	1.384924	8.950784
H	-0.052401	6.013894	7.776118	H	7.775221	2.544652	7.576179
C	0.219872	1.845848	6.575713	C	7.573356	6.792589	8.787784

H	-0.054303	2.912563	6.524276	H	7.839687	5.725530	8.713967
H	-0.327766	1.372050	7.403713	H	8.111640	7.348016	8.006205
H	-0.055473	1.361371	5.625673	H	7.871085	7.170784	9.778175
C	0.045278	8.262798	10.419947	C	7.389468	-0.042784	4.844887
H	0.506921	8.946338	9.690883	H	6.850387	-0.647059	5.588081
H	-0.263474	8.807286	11.318815	H	7.505870	-0.581618	3.898055
H	-0.839007	7.828777	9.927749	H	8.385232	0.160560	5.269964
C	0.730625	6.350931	3.327183	C	7.137655	2.320184	11.992450
H	0.704072	6.154148	2.240250	H	7.233641	2.469523	13.082540
H	0.298608	7.351303	3.507369	H	7.578692	1.341757	11.735262
H	0.079196	5.603503	3.815515	H	7.723715	3.110883	11.492417
C	3.720836	5.409738	1.262933	C	4.153485	3.171773	14.169018
H	3.104183	4.575209	0.899395	H	4.729570	4.029929	14.548609
H	4.509854	5.645202	0.531921	H	3.367997	2.897779	14.890453
H	3.080498	6.296696	1.373953	H	4.837080	2.315162	14.064731
C	0.301961	0.771675	10.466937	C	7.386215	7.794536	5.047923
C	0.676422	1.891558	1.840254	C	7.174688	6.749053	13.605524
H	-0.171653	2.556469	1.624387	H	7.959728	6.036439	13.892662
H	0.321775	0.890708	2.109782	H	7.610783	7.709264	13.308649
H	1.290634	1.835566	0.929192	H	6.526996	6.897390	14.482952
C	0.530882	3.824297	14.485577	C	7.364720	4.643512	0.946813
C	4.313052	8.474529	2.805790	C	3.504155	0.165971	12.603096
O	5.059780	7.943707	1.962748	O	2.802155	0.576863	13.535170
C	3.701356	7.833629	13.361406	C	4.114820	0.873477	2.130634
H	3.607094	7.880974	12.272986	H	4.180201	0.809336	3.218882
C	-0.493142	3.818567	15.591155	C	8.427899	4.524471	-0.116895
H	-0.119310	4.375499	16.460840	H	8.217150	3.686038	-0.792431
H	-0.762309	2.792471	15.867811	H	8.523693	5.467242	-0.670061
H	-1.394244	4.340410	15.232447	H	9.390185	4.326331	0.381407
C	0.495961	10.948611	6.413845	C	7.274599	-2.237103	9.127884
H	-0.488667	10.755990	6.866415	H	8.277039	-2.008620	8.734169
H	0.369292	11.217886	5.359022	H	7.358251	-2.530832	10.180752
H	0.946690	11.782497	6.970566	H	6.873439	-3.064591	8.526418
C	3.390595	6.557198	15.260908	C	4.479727	2.164077	0.253582
H	3.007493	5.620538	15.670276	H	4.876444	3.098032	-0.144772
C	4.225304	8.885793	14.104750	C	3.599400	-0.166013	1.366074
H	4.543277	9.798070	13.597548	H	3.260865	-1.078043	1.860577
C	4.338094	8.745846	15.485348	C	3.519565	-0.016977	-0.016186
H	4.747593	9.553978	16.096203	H	3.118559	-0.815994	-0.644069
C	3.153788	-0.541927	5.333928	C	4.656858	9.209629	10.177411
H	3.818383	-1.383376	5.598269	H	3.989297	10.055732	9.934055
H	2.847386	-0.662786	4.280226	H	4.982671	9.319807	11.226505
H	2.241492	-0.606811	5.949083	H	5.558548	9.284291	9.547379
C	3.395425	9.599558	2.427189	C	4.410571	-1.017485	12.742093
H	2.361691	9.220382	2.441200	H	4.368927	-1.412743	13.763023
H	3.633188	9.981745	1.427965	H	4.108208	-1.794310	12.024390
H	3.448927	10.401178	3.176411	H	5.437702	-0.731633	12.474460
C	3.916344	7.554966	16.073262	C	3.966055	1.177235	-0.578400
H	3.980110	7.398693	17.151512	H	3.930680	1.346831	-1.656008
O	0.528719	0.984200	11.672891	O	7.232639	7.578308	3.834208
C	-0.759016	-0.237329	10.104467	C	8.428274	8.798753	5.468778
H	-1.119535	-0.767376	10.993476	H	8.789634	9.369027	4.605464

H -0.358563 -0.948738 9.367824	H 8.016813 9.472058 6.233410
H -1.599520 0.286180 9.623317	H 9.273162 8.261561 5.927080

Table S11. Cartesian coordinates of [Mn₁₈-Piv].

Total energy: -27090.917966193294 Hartree.

Atom	X	Y	Z	Atom	X	Y	Z
Mn	6.080821	21.652887	4.731320	H	1.984152	14.772056	8.754526
Mn	3.646437	16.911260	3.858054	C	-1.421618	23.402882	6.472129
Mn	1.300953	22.924304	5.641274	H	-1.183958	24.462464	6.281031
Mn	5.235066	19.368219	2.716043	H	-2.120282	23.348269	7.323092
Mn	0.334392	20.842439	3.743926	H	-1.897568	22.978408	5.575124
Mn	2.195356	19.206812	2.426576	C	1.140540	24.422160	9.508630
Mn	0.353628	21.257014	10.069365	H	0.487892	25.293279	9.325076
Mn	-0.370717	20.627935	6.773145	H	1.411962	24.424006	10.574479
Mn	8.079644	18.779209	4.528163	H	2.053243	24.520824	8.901950
Mn	2.623280	20.886908	7.229835	C	-1.379217	19.509830	0.126026
Mn	4.352109	18.901783	8.461455	C	0.175117	23.737384	3.048268
Mn	3.995232	23.233297	6.159969	H	0.045161	24.730490	3.509693
Mn	5.533093	21.199839	7.580678	H	-0.692777	23.543684	2.394780
Mn	4.740253	19.217035	5.585718	H	1.088482	23.749169	2.430176
Mn	3.188063	21.263866	4.196508	C	7.761704	17.754257	-0.831349
Mn	3.346892	16.835594	6.633456	H	8.242488	17.677370	-1.819453
Mn	1.668083	18.780333	5.257927	H	6.742082	18.141717	-0.969752
Mn	1.176176	18.383535	8.412391	H	7.690293	16.738304	-0.413730
O	2.810631	18.573345	9.706502	C	8.725738	21.731974	3.596501
O	5.656452	19.092074	9.912771	C	-0.743045	18.928833	-1.133099
O	3.960841	20.735193	8.516824	H	-0.147055	18.035367	-0.903075
O	4.504532	17.010099	8.165997	H	-0.074904	19.657680	-1.615681
O	2.889526	23.028149	4.643552	H	-1.527817	18.653507	-1.854420
O	2.450445	22.706494	7.157765	C	3.772406	19.617938	-0.012257
O	5.583692	23.469515	5.086408	H	4.816283	19.674243	-0.364226
O	3.065196	18.886331	6.805873	H	3.260190	20.553388	-0.296472
O	6.572636	21.026310	9.221423	H	3.273587	18.776431	-0.528071
O	5.129364	23.088118	7.715875	C	9.766915	22.620082	2.905445
O	2.214165	16.980609	5.109523	C	3.498614	27.767038	6.429949
O	4.824126	21.589639	3.224784	H	3.367708	28.859563	6.392709
O	4.416290	21.244756	5.863434	H	4.313258	27.488766	5.747118
O	1.818730	16.634805	7.876479	H	3.811940	27.489665	7.447018
O	1.078414	20.278715	8.308606	C	-2.532465	20.891931	8.815521
O	1.968681	21.043803	2.790787	C	7.418007	15.640011	4.173181
O	5.702579	19.319178	7.202230	H	7.589627	15.920888	3.122329
O	7.546978	22.205834	3.641044	H	6.543228	14.972957	4.207606
O	3.762205	19.443621	1.371160	H	8.296552	15.088104	4.547046
O	-0.245932	22.693354	6.787826	C	10.960753	21.774311	2.469564
O	3.485349	19.334396	4.031454	H	11.406542	21.249307	3.325515
O	1.553011	20.829767	5.468067	H	11.728798	22.412276	2.005608
O	0.812753	19.308344	1.041558	H	10.661621	21.010435	1.737340
O	5.138931	17.150600	2.764804	C	10.216028	23.662196	3.939887
O	-0.657108	20.658165	2.082957	H	9.360108	24.239787	4.319818
O	0.074531	18.501595	6.748150	H	10.927613	24.364977	3.478682
O	6.193306	19.732324	4.504902	H	10.718476	23.185151	4.795491
O	-1.142017	20.581889	4.917928	C	-4.035464	20.809554	9.109936
O	7.019035	21.567751	6.421807	C	-2.259031	18.448783	0.807304
O	6.743749	19.483313	1.357977	H	-3.043508	18.110480	0.112438

O	0.473424	23.224564	9.224168	H	-2.742427	18.860529	1.704592
H	0.293690	23.122374	8.245642	H	-1.665061	17.572534	1.108976
O	-2.141489	20.376981	7.739866	C	-2.222582	20.739107	-0.210448
O	-0.362524	19.454828	11.098799	H	-1.617944	21.509831	-0.710456
O	8.274048	18.270961	2.434993	H	-2.652347	21.181554	0.698301
O	-1.783672	21.488579	9.628896	H	-3.042212	20.456683	-0.889126
O	9.077635	20.651605	4.092259	C	-2.377863	20.087314	4.510632
O	2.235668	20.774181	11.014664	H	-3.011480	19.914145	5.396654
H	2.568107	19.993375	10.485863	H	-2.893809	20.802040	3.844001
O	4.730454	17.316241	5.411377	H	-2.276161	19.132174	3.962581
O	3.516025	25.102837	6.295391	C	-4.325387	21.186662	10.559572
O	1.323906	24.878315	5.829050	H	-3.789426	20.525300	11.255825
O	3.637370	14.932739	6.444263	H	-5.403505	21.103074	10.767466
O	2.433802	17.260311	2.367376	H	-4.017392	22.221393	10.768909
O	-0.619109	22.370405	11.801491	C	8.728287	17.833451	7.552892
H	-1.448881	22.299164	11.291096	H	8.210047	17.787716	8.523435
O	-0.135668	17.700324	9.748089	H	8.623579	16.854493	7.056179
O	3.843571	14.821544	4.217953	H	9.797340	18.014055	7.748097
O	0.233838	22.762221	4.048194	C	-4.731200	21.792141	8.158513
O	0.743641	18.967981	3.707928	H	-4.408784	22.827343	8.351444
O	7.212152	16.777908	4.974423	H	-5.823138	21.746420	8.296460
H	6.227861	16.915164	5.121766	H	-4.501739	21.550204	7.110548
O	8.214096	18.871400	6.761426	C	-0.303874	17.373922	13.128299
H	7.260852	19.056437	7.012190	H	-0.768026	16.775202	13.927517
N	10.278609	18.107190	4.664909	H	-0.168951	18.402358	13.492140
C	10.804086	17.208955	3.832276	H	0.690998	16.948843	12.924810
H	10.092872	16.632012	3.236891	C	-1.326369	15.919142	11.360669
C	12.178070	17.029627	3.696316	H	-1.813488	15.291252	12.122768
H	12.565094	16.284361	2.999320	H	-0.343570	15.483447	11.131334
C	13.030835	17.826869	4.454726	H	-1.929623	15.881067	10.442179
H	14.114926	17.718544	4.369218	C	-4.519377	19.387014	8.818943
C	12.478985	18.770443	5.318861	H	-4.317915	19.112264	7.774777
H	13.109239	19.421388	5.927430	H	-5.601895	19.305705	9.004607
C	11.093835	18.876303	5.389527	H	-4.008882	18.653607	9.461700
H	10.604967	19.610528	6.036300	C	-0.308724	19.864072	1.160490
C	2.358970	25.554361	6.069593	C	3.300784	21.483299	11.586518
C	3.013349	17.582649	10.687651	H	4.075390	21.706077	10.838301
H	2.995870	16.577042	10.240124	H	3.751790	20.915834	12.420158
H	2.230749	17.656705	11.460335	H	2.915065	22.430208	11.992854
H	3.994355	17.733565	11.166651	C	7.431037	20.051009	11.205242
C	3.981381	12.788639	5.488128	C	5.685553	16.270475	8.273315
C	6.473823	20.048012	10.010574	H	6.322650	16.400232	7.384001
C	7.131381	21.308830	12.030046	H	5.441619	15.200551	8.374386
H	6.103129	21.292180	12.420630	H	6.242832	16.591756	9.168565
H	7.253838	22.214094	11.418862	C	3.804335	14.304476	5.352331
H	7.819415	21.368440	12.887420	C	8.581569	18.676976	0.079746
C	-0.515432	18.253478	10.829481	C	7.240210	18.800039	12.055872
C	5.212592	12.535607	6.365743	H	6.216817	18.739488	12.452774
H	5.375733	11.452996	6.484229	H	7.940921	18.812616	12.904770
H	5.080394	12.979588	7.362324	H	7.420993	17.886789	11.470789
H	6.120228	12.967658	5.915529	C	2.195274	27.075635	6.043128
C	8.694248	20.052969	-0.580295	C	5.949010	24.653267	4.449157

H	9.319142	20.732017	0.017928	H	6.264829	25.405967	5.193180
H	7.701931	20.511246	-0.689544	H	5.107254	25.072924	3.871764
H	9.156139	19.961669	-1.575932	H	6.786581	24.460873	3.761428
C	-0.791316	21.814353	13.083867	C	-1.185928	17.348490	11.873495
H	-1.181598	20.786500	13.029724	C	1.802712	27.449643	4.607231
H	-1.459530	22.436404	13.703586	H	0.852994	26.974461	4.324977
H	0.193806	21.779263	13.569857	H	2.572013	27.128973	3.887627
C	4.861107	22.505635	2.148191	H	1.689009	28.541474	4.522214
H	4.322130	23.426633	2.412890	C	7.999291	22.486971	6.800343
H	4.373280	22.064113	1.270955	H	8.931164	22.287093	6.247832
H	5.910541	22.736483	1.916341	H	8.208447	22.378440	7.876713
C	4.168740	12.151405	4.115152	H	7.670672	23.522979	6.611941
H	5.061081	12.548788	3.610563	C	5.178439	16.459785	1.551950
H	3.306637	12.351877	3.463493	H	4.881021	15.402828	1.685873
H	4.283356	11.061151	4.218110	H	6.210383	16.463080	1.163809
C	2.733335	12.222741	6.173800	H	4.515968	16.915867	0.796985
H	2.836520	11.134620	6.308214	C	-2.560584	17.931487	12.209854
H	1.830696	12.404700	5.569615	H	-3.218964	17.941871	11.328626
H	2.585361	12.685007	7.159698	H	-2.471232	18.962614	12.579256
C	7.816780	18.823437	1.406984	H	-3.048071	17.324881	12.988578
C	8.865349	20.124139	10.669328	C	1.311422	16.429151	2.214807
H	9.574815	20.181670	11.509158	H	1.636717	15.375877	2.163994
H	8.999938	21.010358	10.034030	H	0.798186	16.678692	1.271829
H	9.116984	19.235515	10.072187	H	0.601702	16.545830	3.050209
C	4.814974	23.702053	8.926981	C	9.133788	23.329696	1.707421
H	4.701412	24.789007	8.774498	H	8.706560	22.610626	0.993664
H	5.628167	23.534455	9.653598	H	9.891848	23.930090	1.180738
H	3.875049	23.303881	9.342477	H	8.323076	23.998342	2.026661
C	1.071693	27.468353	7.006488	C	-0.891384	17.525466	6.426994
H	0.882757	28.551079	6.942780	H	-1.702879	17.531549	7.172206
H	1.340561	27.233734	8.047842	H	-0.429981	16.527084	6.386529
H	0.141946	26.935654	6.762166	H	-1.312282	17.749529	5.435806
C	9.965233	18.080149	0.313682	O	2.209756	22.653471	0.580135
H	9.891840	17.075530	0.754049	H	2.073303	22.048290	1.341647
H	10.558915	18.700438	1.001473	C	1.137454	22.562265	-0.299793
H	10.511194	17.999428	-0.639626	H	1.287285	23.291802	-1.111789
C	1.268111	15.381891	8.176256	H	0.166250	22.793271	0.177936
H	1.024256	14.832041	7.251997	H	1.049847	21.562730	-0.771099
H	0.350393	15.510143	8.771047				

References

1. SAINT, 2016.
2. SADABS, 2016.
3. G. Sheldrick, *Acta Crystallogr. Sect. A*, 2015, **71**, 3-8.
4. G. Sheldrick, *Acta Crystallogr. Sect. C*, 2015, **71**, 3-8.
5. K. L. Taft, A. Caneschi, L. E. Pence, C. D. Delfs, G. C. Papaefthymiou and S. J. Lippard, *J. Am. Chem. Soc.*, 1993, **115**, 11753-11766.
6. G. L. Abbatì, A. Cornia, A. C. Fabretti, A. Caneschi and D. Gatteschi, *Inorg. Chem.*, 1998, **37**, 3759-3766.
7. H. J. Eppley, S. M. J. Aubin, W. E. Streib, J. C. Bollinger, D. N. Hendrickson and G. Christou, *Inorg. Chem.*, 1997, **36**, 109-115.
8. E. K. Brechin, J. C. Huffman, G. Christou, J. Yoo, M. Nakano and D. N. Hendrickson, *Chem. Commun.*, 1999, 783-784.
9. D. J. Price, S. R. Batten, B. Moubaraki and K. S. Murray, *Chem. Commun.*, 2002, 762-763.
10. A. Vinslava, A. J. Tasiopoulos, W. Wernsdorfer, K. A. Abboud and G. Christou, *Inorg. Chem.*, 2016, **55**, 3419-3430.
11. A. J. Tasiopoulos, A. Vinslava, W. Wernsdorfer, K. A. Abboud and G. Christou, *Angew. Chem. Int. Ed.*, 2004, **43**, 2117-2121.
12. R. Sessoli, H. L. Tsai, A. R. Schake, S. Wang, J. B. Vincent, K. Folting, D. Gatteschi, G. Christou and D. N. Hendrickson, *J. Am. Chem. Soc.*, 1993, **115**, 1804-1816.
13. S. M. J. Aubin, Z. Sun, H. J. Eppley, E. M. Rumberger, I. A. Guzei, K. Folting, P. K. Gantzel, A. L. Rheingold, G. Christou and D. N. Hendrickson, *Inorg. Chem.*, 2001, **40**, 2127-2146.
14. S. Mukherjee, K. A. Abboud, W. Wernsdorfer and G. Christou, *Inorg. Chem.*, 2013, **52**, 873-884.
15. S. K. Langley, R. A. Stott, N. F. Chilton, B. Moubaraki and K. S. Murray, *Chem. Commun.*, 2011, **47**, 6281-6283.
16. T. C. Stamatatos, K. A. Abboud, W. Wernsdorfer and G. Christou, *Angew. Chem. Int. Ed.*, 2008, **47**, 6694-6698.
17. M. Soler, W. Wernsdorfer, K. Folting, M. Pink and G. Christou, *J. Am. Chem. Soc.*, 2004, **126**, 2156-2165.
18. J. T. Brockman, J. C. Huffman and G. Christou, *Angew. Chem. Int. Ed.*, 2002, **41**, 2506-2508.
19. N. E. Chakov, L. N. Zakharov, A. L. Rheingold, K. A. Abboud and G. Christou, *Inorg. Chem.*, 2005, **44**, 4555-4567.
20. D. I. Alexandropoulos, A. Fournet, L. Cunha-Silva, G. Christou and T. C. Stamatatos, *Inorg. Chem.*, 2016, **55**, 12118-12121.
21. C. Lampropoulos, C. Koo, S. O. Hill, K. Abboud and G. Christou, *Inorg. Chem.*, 2008, **47**, 11180-11190.
22. A. E. Thuijs, P. King, K. A. Abboud and G. Christou, *Inorg. Chem.*, 2015, **54**, 9127-9137.
23. T. C. A. Stamatatos, Khalil A, W. Wernsdorfer and G. Christou, *Angew. Chem. Int. Ed.*, 2007, **46**, 884-888.

24. J. Yoo, A. Yamaguchi, M. Nakano, J. Krzystek, W. E. Streib, L.-C. Brunel, H. Ishimoto, G. Christou and D. N. Hendrickson, *Inorg. Chem.*, 2001, **40**, 4604-4616.
25. M. Murugesu, W. Wernsdorfer, K. A. Abboud and G. Christou, *Angew. Chem. Int. Ed.*, 2005, **44**, 892-896.
26. T. C. Stamatatos, D. Foguet-Albiol, W. Wernsdorfer, K. A. Abboud and G. Christou, *Chem. Commun.*, 2011, **47**, 274-276.
27. D. N. Hendrickson, G. Christou, E. A. Schmitt, E. Libby, J. S. Bashkin, S. Wang, H. L. Tsai, J. B. Vincent and P. D. W. Boyd, *J. Am. Chem. Soc.*, 1992, **114**, 2455-2471.
28. E. K. Brechin, W. Clegg, M. Murrie, S. Parsons, S. J. Teat and R. E. P. Winpenny, *J. Am. Chem. Soc.*, 1998, **120**, 7365-7366.
29. M. C. Biesinger, B. P. Payne, A. P. Grosvenor, L. W. M. Lau, A. R. Gerson and R. S. C. Smart, *Appl. Surf. Sci.*, 2011, **257**, 2717-2730.
30. C. Bosch-Navarro, E. Coronado, C. Martí Gastaldo, B. Rodríguez González and L. M. Liz Marzán, *Adv. Funct. Mater.*, 2012, **22**, 979-988.
31. F. Neese, F. Wenmohs, U. Becker and C. Ripplinger, *J. Chem. Phys.*, 2020, **152**, 224108.
32. J. P. Perdew, K. Burke and M. Ernzerhof, *Phys. Rev. Lett.*, 1997, **78**, 1396-1396.
33. F. Weigend and R. Ahlrichs, *Phys. Chem. Chem. Phys.*, 2005, **7**, 3297-3305.
34. T. Lu and F. Chen, *J. Comput. Chem.*, 2012, **33**, 580-592.
35. A. J. W. Thom, E. J. Sundstrom and M. Head-Gordon, *Phys. Chem. Chem. Phys.*, 2009, **11**, 11297-11304.